# Egyptian Journal of Chemistry

**http://ejchem.journals.ekb.eg/**

## Laboratory study for accelerating the CKD mineral carbonation

**Ahmed Baher, Asmaa S. Hamouda, Ibrahim M. El-Kattan and M.A. Abdelzaher***
*Environmental Science and Industrial Development Department, Faculty of Postgraduate Studies for Advanced Sciences, Beni Suef University, Beni Suef 62511, Egypt*

**Abstract**

Mineral carbonation is one of the typical carbon capture, utilization, and storage technologies, employed to extract synthetic carbonates from metal oxide and $CO_2$. However, the technology is known to be extremely challenging to achieve economic feasibility because expensive chemical solvents used the account for most of the cost. To overcome this limitation, we have conducted a pilot laboratory study to secure the economic viability of the technology by replacing these chemical solvents with costless metallic carbon dioxide cylinders. For the current study, we have implemented cement kiln dust (CKD), an alkali industrial by-product, together with mineral $CO_2$ gas. In this research paper, we attained $CO_2$ storage and $CaCO_3$ yield, which is comparable both quantitatively and qualitatively to currently available studies. With a steady flow rate of 0.9 l/m of carbon dioxide over further more fixed time, the carbonation of CKD could dramatically increase, reaching 35% of calcium carbonate at 550°C and 27% of calcium carbonate at 450°C respectively. It was also found that $CO_2$ flow rate is one component, which can elute Ca from CKD, and had significant effects on carbonation efficiency. The solid to liquid ratio was the most influential factor in the Ca elution process. the microstructure, morphology and thermal traits of the designed patches are characterized by using scanning electron microscopy (SEM) to indicate the phase's composition, X-Ray Diffraction (XRD) and Fourier-transform infrared spectroscopy (FTIR) measurements.

**Keywords:** Mineral Carbonation; Cement Kiln Dust; Carbon Capture; Morphology and Phases Composition

## 1. Introduction

Reducing global warming requires almost zero long-term man-made emissions. In other words, while some human works generate huge greenhouse gases into the atmosphere, others remove the same quantity, leading to a net-zero balance. Limiting global warming to 2°C requires reaching net zero emissions by 2100 [1, 2]. Consequently, coal-fired power plants besides a variety of industries, such as cement, steelmaking and petrochemical industries, emit very large quantities of carbon dioxide, contributing to climate change through global warming of the earth. The global $CO_2$ emission from the cement industry was 2.20±0.20 gt $CO_2$ in 2019, which is around 7.8% of the global $CO_2$ emissions [1, 3]. While the global demand for cement is expected to increase by 12 to 23% by 2100, the International Energy Agency (IEA) predicts that direct $CO_2$ emissions from cement production will roughly increase 4% during the same period [4-6]. Many opportunities exist for $CO_2$ emission in the cement industry, with three preferred measures by which $CO_2$ emissions have been mitigated over the last years (e.g.: a) Energy efficiency improvement; b) Fuel switching by using waste as an alternative fuel, and c) Blended cement by reduction of clinker/cement ratio using

industrial by-products [7-9]. The chemical composition of the collected cement kiln dust from the kiln inlet point known as the bypass opening of the vortex varies with different production line processes. The concentration of lime in fresh dust ranges between 42 to 60% with an average of 51.6% [10-12]. Thee amount of chloride and sulfate was about 8.0 and 11.5% maximum. Cement kiln dust is a very fine powder that has the appearance of fly ashes. CKD consists of ultra-fine particles that are collected as mentioned above and during the production of cement clinker. The concentration of lime, sulfate, and alkali in CKD is primarily influenced by the particle size of the materials collected at the kiln inlet [13]. Coarse/heavy particles of CKD have a high content of lime while fine/light particles have a higher concentration of sulfates and alkalis and lower lime content [14, 15]. To further reduce dust emissions from the cement chimneys, $CO_2$ emissions from calcination can be captured and utilized, for example, through mineral carbonation of industrial solid waste. The carbonated materials may then be used as fillers for blended cement production [16, 17]. Cement kiln dust is produced at kiln inlet, with the temperature around 800°C to 1000°C of the clinker [18-20]. The

---

mineral carbonation of CKD (MC) with flue gas containing $CO_2$ is a CCU technology that uses $CO_2$ to form synthetic carbonate materials through the reaction of $CO_2$ and calcium or magnesium-containing species, such as oxides, hydroxides, and silicates [21, 22]. The carbonation reaction is also regulated by the solution balance. As the ions are converted into calcium carbonate and precipitate, more calcium hydroxide is dissolved to maintain the concentration of calcium ions.

Carbon capture is an important strategy for reducing carbon emissions in heavy industries and power plants. It includes two categories: i) carbon capture and storage (CCS); and ii) carbon capture and use (CCU). CCS is a process consisting of separating $CO_2$ emitted by industry power generation facilities, transporting it to a storage place, and isolating it from the long-term atmosphere. In the case of CCU, it involves the conversion of captured $CO_2$ into usable materials, either as an end product or as raw material into a production process [10, 23, 24]. To date, a limited number of studies have explicitly estimated the cost of $CO_2$ avoidance for cement industries. For CCU implementation within the cement plant, post-combustion $CO_2$ capture designs using chemical solvents for cement production, it is evaluated in terms of technical, economic, and environmental aspects to estimate energy and cost fines [25, 26]. Results from that study indicate that implementing post-combustion capture technologies estimated the $CO_2$ avoided cost ranging between 60 and 161 USD/t $CO_2$ [12, 22, 27, 28]. In addition, the total estimated investment cost for $CO_2$ capture in a cement plant ranges between 51 and 294 million United States dollars [29]. However; significant progress in financial analysis for mineral carbonation over the past 10 years, the cost and $CO_2$ abatement potential of this process are not well described in the literature [1, 28, 30]. Previous studies on life cycle assessment do not show economic indicators, a notable gap that should be addressed in further research. Not widely the main accepted indicators emerged [1, 30, 31] and the cost estimate the methods are not fully supported yet. Environmental assessments have the life cycle assessment (LCA) approach is not considered, and indirect $CO_2$ emissions have not been considered, yet, it was included [32, 33]. To make the mineral carbonation process more effective in the direct and indirect reduction of $CO_2$ emissions from the cement production process, further research is needed. Moreover, appraisals can enhance the perfectly integrated evaluation using technical, cost-cutting, environmental, and even outdated fashion indicators, as well as broadly accepted methods. Environmental valuations must include direct and indirect environmental impacts and comparisons with other technologies for emissions abatement are necessary. In our study, we propose a mineral carbonation process where $CO_2$ is captured from the cement plant gas stream, using CKD as raw material to obtain active substances rich in calcium carbonate and calcium sulfate.

We aim to improve the analysis of technological feasibility, economic viability, and environmental impact of mineral carbonation of CKD from $CO_2$-containing flue gas for emissions mitigation in the cement production process. A novel integrated economic and environmental assessment framework is being discussed, in which LCA is conducted in parallel and systematically includes technology maturity. Then, the goal and scope of the current study are presented, including the selection of benchmark processes and scenarios. All input data and assumptions are then described, including the proposed MC process design (section 2). Finally, the analysis and results are presented (section 3).

## 2. Experimental and Methods

### 2.1. Materials Resources and Preparation
The main raw precursors used in this laboratory investigation are cement kiln dust (CKD) and mineral-$Co_2$ cylinder as active gas for carbonation cycle (MC). CKD was brought from Lafarge Egypt Cement Company, (Suez, Egypt). MC was purchased from Al-Rehab Company for Filling and Supplying Cylinders of Medical and Industrial Gases, (Cairo, Egypt). Two kilograms were collected isokinetically from bypass filter screw then homogenized and dried at 105°C for 24 hrs. before usage.

Table 1: Chemical composition of cement kiln dust (CKD)

| Material | SiO$_2$ | Al$_2$O$_3$ | CaO | Fe$_2$O$_3$ | MgO | SO$_3$ | Na$_2$O | K$_2$O | Cl$^-$ | P$_2$O$_5$ |
|----------|---------|-------------|-----|-------------|-----|--------|---------|--------|--------|------------|
| CKD | 14.66 | 4.17 | 46.24 | 2.38 | 0.97 | 1.91 | 5.28 | 4.37 | 9.80 | 0.24 |

The chemical compositions of CKD were determined by the XRF instrument as detailed in (Table 1).

Specific surface area of CKD before MC-process was 5679 $cm^2.gm^{-1}$, also, loss on ignition of CKD was

performed on lab muffle furnace at 950°C for 2hrs recorded 14.92 % weight loss (on a dry basis).

## 2.2. Procedures for absorption and carbonization experiments

Calcination and carbonation cycle of the calcium oxide sorbent present in CKD (CaO scanning rate at 10°C/min), and start heating at the tube glass muffle furnace at different temperature; i.e: 450, 550, 650 and 750°C respectively. After that, start the decarbonisation cycle for $CO_2$ gas to make sure that the material (cement kiln dust) fully composed yield

finishing the decarbonisation and isotherm cycles under $CO_2$ gas to start the carbonation cycle for 60, 90, 120, 180 and 270 seconds respectively. Finally, rapid cooling from required temperature down to 25°C at gas feeding rate 0.30, 0.50, 0.70, and 0.90 l/min, is tested, to reach the optimum active gas flow rate. After that, a part of dried yield was kept for testing with scanning electron microscopy (SEM), X-rays diffraction (XRD), FT-IR spectrum, and a simple laboratory scheme for the experimental program is shown in (Figure 1). The physical properties of the different chemical substances are shown in (Table 2).





$CaCO_3$ in a solid-state, and after that cool down until you reach the required ambient temperature, hence
Figure 1:-. Laboratory diagram for the experimental program

## 2.3. Instrumental Methods

The microstructures (SEM-photos) were obtained with Gemini (Sigma 500 VP, 2020 version). On the other side, another part of the dried sample was milled for 2h to pass from (25 mm sieve mesh) to determine the phases composition by using X-ray diffraction (XRD),

which was carried out using Philips (PW3050/60) diffractometer usiᶦng a scanning range from 5 to 80 (2Ø), with a scanning speed of 1 Se./step and resolution of 0.05 deg. The present oxides that ingested CKD were quantified using X-ray fluorescence performed with a comprehensive instrument Panalytical (*ARL 9900*). The FT-IR was recorded from KBr discussing Genesis-II FT-IR spectrometer in the range of 400–4000 cm⁻¹·

Table 2: The physical properties of the chemical substances [34]

| Molecular Formula | Density | Appearance | Melting Point | Molar Mass | Boiling Point | Solubility in Water |
|---|---|---|---|---|---|---|
| Cao | 3350 kg/m$^3$ | White solid | 2572 °C | 56.1 g/mol | 2850 °C | Reacts |
| $CO_2$ | 1.98 kg/m$^3$ | Colorless gas | -57 °C (under pressure) | 44.0095 g/mol | -78 °C | 1.45kg/m$^3$ |
| $CaCO_3$ | 2.83 g/cm$^3$ | White powder | 825 °C | 100.087 g/mol | Decomposes | Insoluble |

## 3. Results and Discussions

### 3.1. Carbonation Reaction

We conducted a laboratory experimental study to determine the optimal conditions for three variables ($CO_2$ flow rate, timing, and reaction temperature) expected to significantly affect the carbonation efficiency. For the current study, the target variable was varied while the other variables were fixed, i.e: the flow rate varies while the other two variables are constant (reaction temperature and timing) and so on as detailed in (Figures 2a, 2b, 2c, 2d and 2e) respectively. The reactants were continuously mixed during the carbonation reaction process. The composition of the calcium carbonate starts at around 450°C points. Fresh CKD was heated throw different temperatures scale under $CO_2$ gas to ensure that the CKD sample fully decomposed to calcium hydroxide, magnesium carbonate, and calcium carbonate (represented in 5.16% losses of the original sample weight). In addition, the transition accompanied with increment in heat flow rate starts at 450°C till 750°C, and the reaction is repeated at different thermal points (endothermic reaction). Injected $CO_2$ gas flow rate from 0.1 l/m to 0.9 l/m, noticed that CKD gain loss as flow rate increase, which may be attributed to the formation of carbonate and other minerals as detailed in (figure 2a). The same concept, with time, speeds up from 30 sec. up to 270 sec. weight gain of CKD increases as shown in all figures, as the formation of carbonate is proved by XRD and SEM morphology. Finally, the flow automatically was switched on pure calcium carbonate stream to start the carbonation cycle for different time scale, flow rate and temperature [33, 35]. This transition is accompanied by a gain in the sample weight i.e: calcium carbonate yield. Temperature is the main controller in that process, increasing thermal load up to 750°C weight gain of CKD decreases as shown in all figures. Weight loss in CKD may be due to the losses at the main sample weight under the effect of thermal load. The formation of carbonate which is proved by XRD and SEM morphology is increased at CKD-450°C/-550°C respectively.
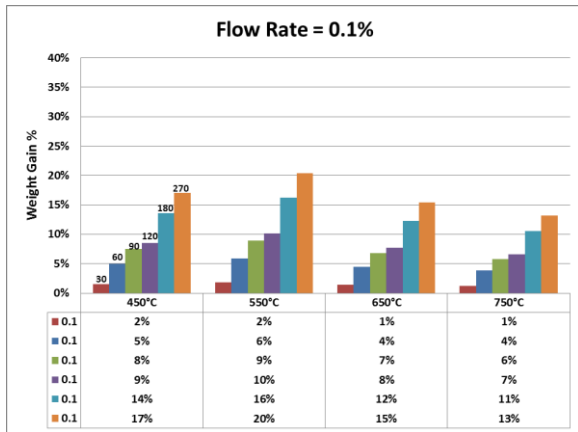
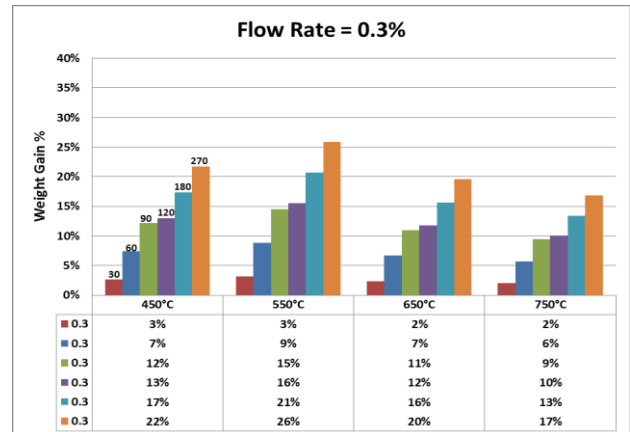Figure 2a:  Effect of flow rate 0.1% on weight gain of CKD



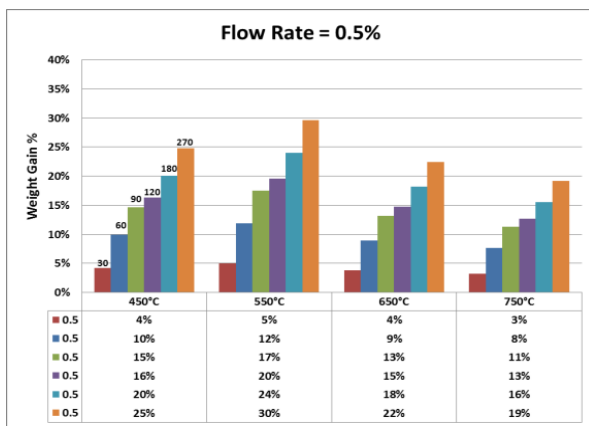Figure 2b:  Effect of flow rate 0.3% on weight gain of CKD



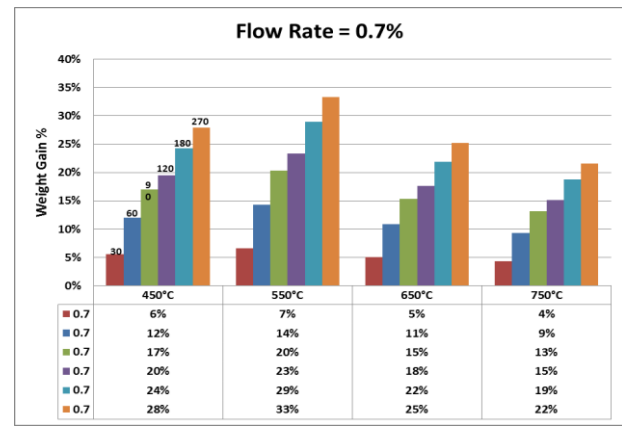Figure 2c:  Effect of flow rate 0.5% on weight gain of CKD



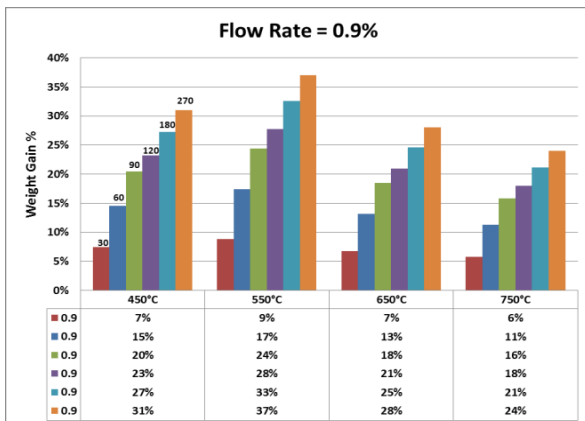Figure 2d:  Effect of flow rate 0.7% on weight gain of CKD



Figure 2e:  Effect of flow rate 0.9% on weight gain of CKD

### 3.2. XRD and Phase Clarification

The interaction of CKD with mineral-$CO_2$ at different thermal condition yields different phases can be clarified by XRD patterns as shown in (figure 3). It denotes the formation of various crystal peaks subordinate to calcium silicate hydrate (C–S–H), calcium carbonate ($CaCO_3$), and mullite ($3Al_2O_3 \cdot 2SiO_2$). CKD is known as a cement by-product; contains the undesirable alkalis in cement kiln environment and high percentile of CaO, $SiO_2$, MgO, etc….. Other alkaline components as detailed at the XRF analysis and explains the absence of portlandite phase. The decrease in calcium silicate hydrate (C-S-H) peak intensity at the CKD with time confirms that the rate of mineral carbonation reaction is ongoing with thermal load, resulting in the formation of calcite and/or mullite phase. However, further formation of these phases over time cannot be demonstrated by XRD as the peak of calcium carbonate overlaps with that of C–S–H and/or C-A-S-H [18, 20, 22, 36]. This perfectly highlights CKD's highly effective surface area in accelerating the

rate of carbonization reaction at a low time scale and/or low mineral-$CO_2$ flow rate. At 550°C, XRD patterns are completely different from those at 450°C because it represents the eutectic heat point where the degree of carbonization increased at that point.
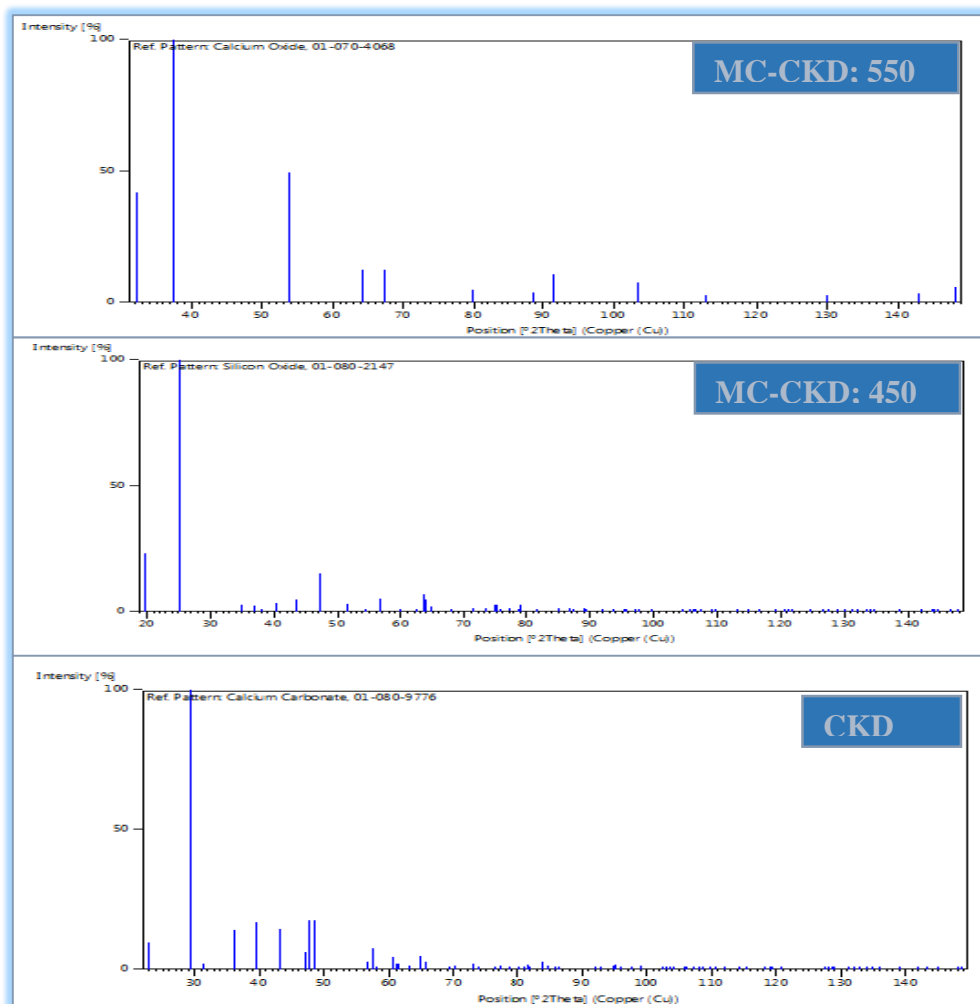


Figure 3. XRD-patterns of CKD 450°C/-550°C

## 3.3. Morphology and Microstructure

The morphology and microstructure of the carbonated CKD particles compared to CKD as received after the drying process are shown in (figure 4) as a function of temperature. The CKD particles were typically ecospheres, which are generally present in ashes, ultra-fine particles, and some vesicular particles may be caused by the presence of gases and vapors. In both the carbonation path, the presence of quasi-cubic structures of calcite was seen as the highlight of the circle. Also, it shows a single calcite particle formed in the thermal carbonation process at 450°C, where at 550°C many calcite particles appear and further magnification of the cross-section of the sample proves the formation of calcite in quasi-cubic structures yields 27% and 32% weight gain respectively. It has been reported that the carbonated CKD particles showed the presence of calcite as the major product, which is also observed in the XRD analysis as explained in Section 3.2. Moreover, the additional thermal carbonation of CKD can produce calcite but in low proportions as CKD begins to lose a fraction of its original weight as the loss upon ignition

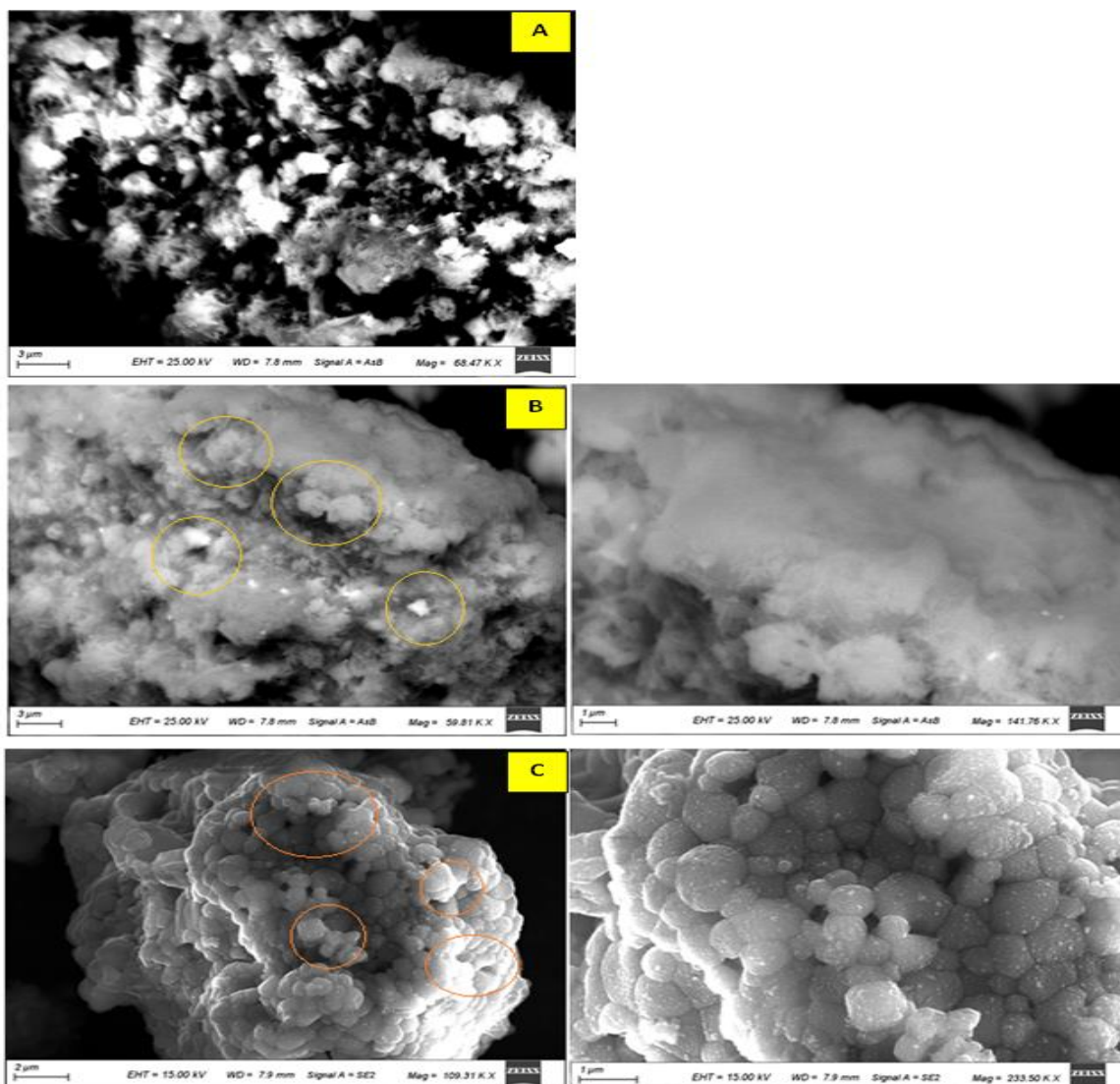and the mineral carbonation process does not occur as expected [37-39].



Figure 4. SEM morphology of CKD as received and MC- CKD-450°C/-550°C

### 3.4. FT-IR Spectroscopy

The functional groups were determined by FTIR analysis. In samples that reflect a higher yield of carbonate products at CKD 450°C/550°C, carbonates were found at $1421cm^{-1}$ and $872$ $cm^{-1}$. As figure (5) shows, $CaCO_3$ and $MgCO_3$ go within the same band. Some differences can be identified using XRD and SEM analysis [38, 40]. The weight loss of CKD-450°C/-550°C would be simultaneously attributed to the decomposition of carbonates (release $CO_2$) and hydrates (release $H_2O$). Therefore, weight loss during thermal degradation was correlated with the evolved

gas of volatiles and/or gases released. The content of chlorides (halite, sylvite, and calcium hydroxyl chloride) positively correlated to the ratio of CKD residues in the mixture, since CKD is mainly contained in high ratios of alkalis [36-38]. The phase compositions of the granules also revealed $CaCO_3$ as a new formation, which may have some role in increasing the weight gain of the samples. Other functional groups, such as S-H & N-H components, appear at $2514cm^{-1}$ & $2377cm^{-1}$ respectively, while the carboxyl group appears at $1421cm^{-1}$.
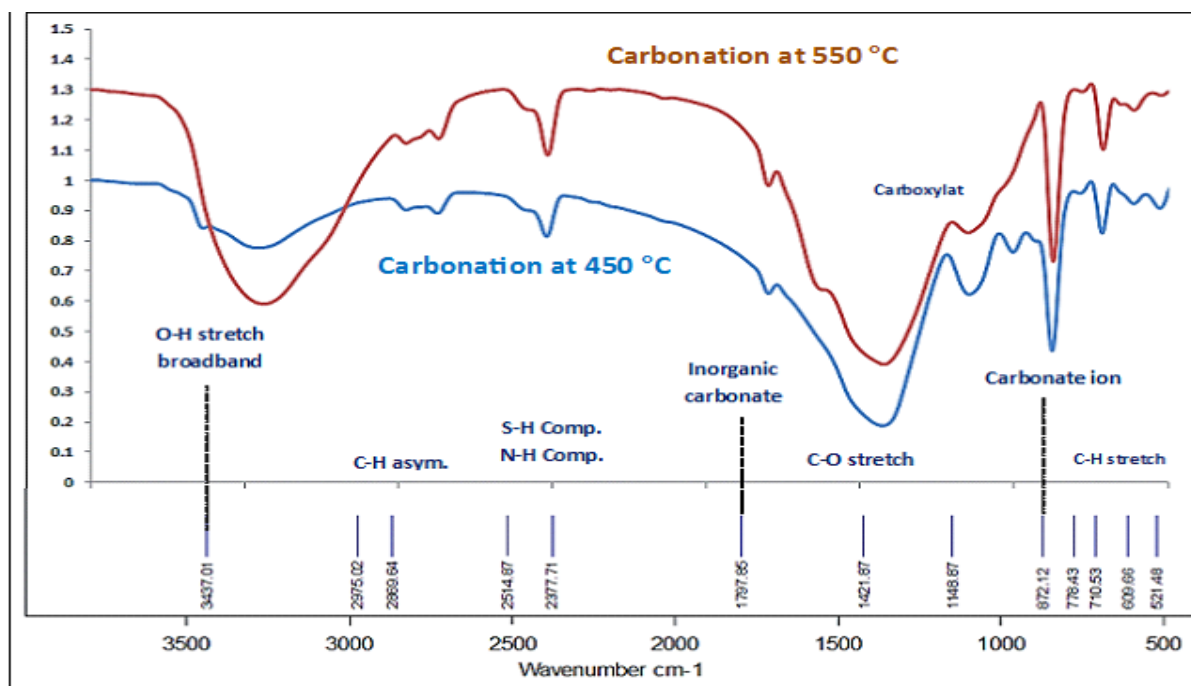
Figure 5: FTIR Analysis of CKD-450°C/-550°C

## 4. Conclusion

This research paper demonstrates the importance of mineral carbonation instead of CKD landfill. Experiments were carried out in core fractions of CKD waste under different operating conditions ($CO_2$ gas input rate, timing, and temperature). The results indicate:

1. The importance of combining economic and environmental aspects to evaluate the performance of MC technologies so that they are applicable in the cement sector.
2. The cost of $CO_2$ captured can be reduced by 32% by implementing MC for CKD.
3. The calcium capture from CKD is suitable for cement production from a net zero emissions perspective and can be used as cement additive materials.
4. The carbonated CKD particles showed the presence of calcite as the major product in both crystalline and amorphous forms, which is also observed in the XRD.
5. Sustainability and innovations are the vision of all policies and regulations for a safe environment. Further practical studies on CKD management should take place. In addition, for reducing $CO_2$ abatement, future research would need to include further LCA impact factors to achieve a fully combined assessment.

## Conflict of Interest

There is no conflict of interest

## References

1. Pedraza, J., et al., *On the road to net zero-emission cement: Integrated assessment of mineral carbonation of cement kiln dust.* 2021. **408**: p. 127346.
2. Jeon, J. and M.-J.J.C.E.J. Kim, *CO2 storage and CaCO3 production using seawater and an alkali industrial by-product.* 2019. **378**: p. 122180.
3. Change, I.J.E.P., *Mitigation of climate change. Contribution of Working Group III to the Fifth Assessment Report of the Intergovernmental Panel on Climate Change, 1454.* 2014. **147**.
4. Awasthi, A.K., et al., *Zero waste approach towards a sustainable waste management.* 2021. **3**: p. 100014.
5. Kajaste, R. and M.J.J.o.c.p. Hurme, *Cement industry greenhouse gas emissions– management options and abatement cost.* 2016. **112**: p. 4041-4052.
6. Heubaum, H. and F.J.E.P. Biermann, *Integrating global energy and climate governance: The changing role of the*

*International Energy Agency.* 2015. **87**: p. 229-239.

7.   Salas, D.A., et al., *Environmental impacts, life cycle assessment and potential improvement measures for cement production: a literature review.* 2016. **113**: p. 114-122.

8.   Saleh, H., et al., *Current situation and future prospects for plastic waste in maysan governorate: effects and treatment during the COVID-19 pandemic.* 2021. **64**(8): p. 4449-4460.

9.   El-Kattan, I.M., et al., *Positive impact of ultra fine-ceramic waste on the physico-mechanical features and microstructure of white cement pastes composites.* 2020. **9**(4): p. 9395-9402.

10.  Peethamparan, S., et al., *Influence of chemical and physical characteristics of cement kiln dusts (CKDs) on their hydration behavior and potential suitability for soil stabilization.* 2008. **38**(6): p. 803-815.

11.  Tantawy, M., et al., *Fire resistance of sewage sludge ash blended cement pastes.* 2013. **2013**.

12.  Chaunsali, P., S.J.C. Peethamparan, and c. research, *Evolution of strength, microstructure and mineralogical composition of a CKD–GGBFS binder.* 2011. **41**(2): p. 197-208.

13.  Gupta, R., et al., *Particulate matter and elemental emissions from a cement kiln.* 2012. **104**: p. 343-351.

14.  Mackie, A.L. and M.E.J.W.r. Walsh, *Bench-scale study of active mine water treatment using cement kiln dust (CKD) as a neutralization agent.* 2012. **46**(2): p. 327-334.

15.  Kim, M.-J., S.J.E.S. Jung, and P. Research, *Calcium elution from cement kiln dust using chelating agents, and CO 2 storage and CaCO 3 production through carbonation.* 2020. **27**(16): p. 20490-20499.

16.  Osmanovic, Z., et al., *Properties of blastfurnace cements (CEM III/A, B, C) based on Portland cement clinker, blastfurnace slag and cement kiln dusts.* 2018. **91**: p. 189-197.

17.  Pan, S.-Y., et al., *An innovative approach to integrated carbon mineralization and waste utilization: A review.* 2015. **15**(3): p. 1072-1091.

18.  Dorado-Bustamante, K., S. Leal-Marin, and H.J.D. Estupiñán-Duran, *Electrochemical analysis of the degradation of nitrided zirconia 3Y-TZP.* 2018. **85**(206): p. 9-15.

19.  Abdelzaher, M.J.E.R.E., *Experiential investigation on the effect of heavy fuel oil substitution by high sulfur petcoke on the physico-mechanical features and microstructure of white cement composites.* 2021. **3**(1): p. 015028.

20.  Elkhouly, H.I., et al., *Experimental and Modeling Investigation of Physicomechanical Properties and Firing Resistivity of Cement Pastes Incorporation of Micro-Date Seed Waste.* 2021: p. 1-13.

21.  Bertos, M.F., et al., *A review of accelerated carbonation technology in the treatment of cement-based materials and sequestration of CO2.* 2004. **112**(3): p. 193-205.

22.  Ukwattage, N., P. Ranjith, and X.J.M. Li, *Steel-making slag for mineral sequestration of carbon dioxide by accelerated carbonation.* 2017. **97**: p. 15-22.

23.  Ncongwane, M.S., J. Broadhurst, and J.J.I.J.o.G.G.C. Petersen, *Assessment of the potential carbon footprint of engineered processes for the mineral carbonation of PGM tailings.* 2018. **77**: p. 70-81.

24.  Shawkey, M.A., et al., *Monitoring of acoustic emission behaviour during early-age cement paste hydration.* IOP Conference Series: Materials Science and Engineering, 2021. **1046**(1): p. 012020.

25.  Cormos, C.-C., A.-M. Cormos, and L. Petrescu, *Assessing the CO2 emissions reduction from cement industry by carbon capture technologies: conceptual design, process integration and techno-economic and environmental analysis*, in *Computer Aided Chemical Engineering*. 2017, Elsevier. p. 2593-2598.

26.  Abbas, R., et al., *Environmental safe disposal of cement kiln dust for the production of geopolymers %J Egyptian Journal of Chemistry.* 2021. **64**(12): p. 7529-7537.

27.  Lee, J.H., et al., *Techno-economic and environmental evaluation of CO2 mineralization technology based on bench-scale experiments.* 2018. **26**: p. 522-536.

28.  Muslemani, H., et al., *A Review of Business Models for Carbon Capture, Utilisation and Storage Technologies in the Steel Sector: A Qualitative Multi-Method Study.* 2019.

29.  Tantawy, M., et al., *Evaluation of the pozzolanic activity of sewage sludge ash.* 2012. **2012**.

30.  Zimmermann, A.W. and R.J.E.T. Schomäcker, *Assessing Early-Stage CO2 utilization Technologies—Comparing Apples and Oranges?* 2017. **5**(6): p. 850-860.

31.  El-Roudi, A., B. Balboul, and M.J.I.J. Abdelzaher, *Influence of limestone on physico-chemical properties of white portland cement pastes.* 2015. **3**(6): p. 210-221.

32.  Schaffert, J., et al., *Innovative large-scale energy storage tech-nologies and power-to-gas concepts after optimisation.* 2020.

33.  Velts, O., et al., *CO2 mineralisation: Production of CaCO3-type material in a continuous flow disintegrator-reactor.* 2014. **63**: p. 5904-5911.

34.  Abunowara, M. and M. Elgarni, *Carbon Dioxide Capture from Flue Gases by Solid Sorbents.* Energy Procedia, 2013. **37**: p. 16-24.

35.  Zhang, B., et al., *Study on the Preparation and Anti-CO2 Corrosion Performance of Soap-Free Latex for Oil Well Cement.* 2020. **5**(36): p. 23028-23038.

36.  Huntzinger, D.N., et al., *Carbon dioxide sequestration in cement kiln dust through mineral carbonation.* 2009. **43**(6): p. 1986-1992.

37.  Abdelzaher, M.A., et al. *Nano titania reinforced limestone cement: physico-mechanical investgation.* in *Key Engineering Materials.* 2018. Trans Tech Publ.

38.  Balboul, B.A., et al., *Nano titania combined with micro silica reinforced limestone cement: physico-mechanical investigation.* 2019. **62**(6): p. 1105-1115.

39.  Wehrmeister, U., et al., *Raman spectroscopy of synthetic, geological and biological vaterite: a Raman spectroscopic study.* 2010. **41**(2): p. 193-201.

40.  Madupalli, H., B. Pavan, and M.M.J.J.o.s.s.c. Tecklenburg, *Carbonate substitution in the mineral component of bone: Discriminating the structural changes, simultaneously imposed by carbonate in A and B sites of apatite.* 2017. **255**: p. 27-35.